Available online at www.sciencedirect.com
SCIENCE DIRECT®
New Astronomy xxx (2004) xxx–xxx
New Astronomy
www.elsevier.com/locate/newast

Near-IR spectroscopy of asteroids 21 Lutetia, 89 Julia, 140 Siwa, 2181 Fogelin and 5480 (1989YK8), potential targets for the Rosetta mission; remote observations campaign on IRTF

Mirel Birlan [a,b,*], Maria Antonietta Barucci [a], Pierre Vernazza [a], Marcello Fulchignoni [a], Richard P. Binzel [c], Schelte J. Bus [d], Irina Belskaya [a,e], Sonia Fornasier [f]

[a] *Observatoire de Paris-Meudon, LESIA, 5 Place Jules Janssen, 92195 Meudon Cedex, CNRS, France*
[b] *Astronomical Institute of the Romanian Academy, Str Cutitul de Argint n 5, Bucharest 28, Romania*
[c] *Department of Earth, Atmospheric and Planetary Sciences, Massachusetts Institute of Technology, Cambridge, MA 02139, USA*
[d] *Institute for Astronomy, 640 North A'ohoku Place, Hilo, HI 96720, USA*
[e] *Astronomical Observatory of Kharkov University, Sumskaya str. 35, Kharkov 310022, Ukraine*
[f] *Astronomical Department of Padova, Vicolo dell'Osservatorio 2, 35122 Padova, Italy*

Received 27 October 2003; received in revised form 5 December 2003; accepted 10 December 2003

Communicated by W.D. Cochran

Abstract

In the frame of the international campaign to observe potential target asteroids for the Rosetta mission, remote observations have been carried out between Observatoire de Paris, in Meudon-France and the NASA Infrared Telescope Facility on Mauna Kea. The SpeX instrument was used in the 0.8–2.5 μm spectral region, for two observing runs in March and June 2003. This paper presents near-IR spectra of the asteroids 21 Lutetia, 89 Julia, 140 Siwa, 2181 Fogelin and 5480 (1989YK8). Near-IR spectra of the asteroids 21 Lutetia and 140 Siwa are flat and featureless. The spectrum of 89 Julia reveals absorption bands around 1 and 2 μm, which may indicate the presence of olivine and olivine-pyroxene mixtures and confirm the S-type designation. The small main-belt asteroids 2181 Fogelin and 5480 (1989YK8) are investigated spectroscopically for the first time. Near-IR spectra of these asteroids also show an absorption feature around 1 μm, which could be and indicator of igneous/metamorphic surface of the objects; new observations in visible as well as thermal albedo data are necessary to draw a reliable conclusion on the surface mineralogy of both asteroids.

* Corresponding author.
E-mail addresses: mbirlan@despace.obspm.fr, mirel.birlan@obspm.fr (M. Birlan).

1384-1076/$ - see front matter © 2003 Elsevier B.V. All rights reserved.
doi:10.1016/j.newast.2003.12.005

PACS: 95.45.+i; 95.85.Jq; 96.30.Ys

Keywords: Methods: miscellaneous; Techniques: spectroscopic; Minor planets: asteroids; Infrared: solar system

1. Introduction

The observational program presented in this paper is intimately linked to the scientific programme of the space mission Rosetta. The Rosetta mission was approved in 1993 as a Cornerstone Mission within the ESA's Horizons 2000 science programme. The original launch date for the mission was January 2003 and the scientific targets were assigned to be the nucleus of comet 46P/Wirtanen and two main-belt asteroids: 140 Siwa and 4979 Otawara. The main scientific goals of the Rosseta mission are to investigate 'in situ' primitive objects of the solar system and to find answers concerning the chemical composition of the primitive planetary nebula, thought to be 'frozen' in the comet nucleus and the asteroid mineralogical matrix.

Since 1993, several international campaigns of observations have been started in order to obtain a large amount of data for the targets of the Rosetta mission (Fornasier et al., 2003; LeBras et al., 2001; Barucci et al., 1998, etc.). The groundbased knowledge of these objects is essential to optimise the science return as well as the mission trajectory.

In January 2003 the European Space Agency decided to postpone the launch of the Rosetta, with a new launch date set to February 2004. This decision implied a new mission baseline: rendezvous with the comet P/Churyumov-Grasimenko and one or two asteroid fly-bys to be defined after the spacecraft interplanetary orbit insertion manoeuvre, when the total amount of available δv will be known. Several fly-bys scenarios have been studied and several possible asteroid targets have been found. These potential targets are poorly known and for this reason systematic observation are needed in order to significantly improve on our knowledge of the physics and the mineralogy of these objects.

In this paper we present the spectroscopic results obtained for five asteroids [21 Lutetia, 89 Julia, 140 Siwa, 2181 Fogelin and 5480 (1989YK8)], potential targets of the Rosetta mission. The 0.8–2.5 μm wavelength region was investigated using the SpeX instrument on IRTF-Hawaii, in 'remote observing' mode.

2. The observing protocol

The remote observations were conducted from Meudon-France, more than 12,000 km away from Hawaii, using several informational structures and networks. For the observers in Meudon, the observing hours occurred during relatively normal working daylight hours. Observation sessions began at 5 a.m. local time and ended at 5 p.m. local time. This type of observations between Meudon and IRTF/Hawaii was started in 2002 (Birlan and Binzel, 2002); since then, more than twenty nights of observations (in eight runs) were conducted from Meudon. The observations were realized through an ordinary network link, without the service quality warranty. Thus, the passband for our link was variable, a function of the traffic between Hawaii and Meudon.

During the remote observing run, the Observatoire de Paris team had the control of both the instrument/guider system and the spectrograph set-up and spectra acquisition. A permanent and constant audio/video link with the telescope operator is essential in order to administrate possible service interruptions. Two PC's running Linux were devoted to the telescope/spectrograph control. The X environment for the telescope and instrument control was exported from Mauna Kea to Meudon via two secure links (ssh tunnels). A third PC was used to keep the IP audio-video link open (webcam/Netmeeting at Meudon and Polycom ViewStation video-conference system on Mauna Kea). All software was re-initialized at the beginning of each night.

The communication lag was relatively small (approximately 0.5 s), and the image refresh time

was 2 s on the average. Real-time image display was performed mainly for verification purposed and preliminary analysis. At the completion of each run, all files were transferred to Meudon.

The SpeX instrument was utilized in low-resolution mode for this campaign. The observations were made in the 0.8–2.5 μm spectral interval. We used a 0.8 arcsec wide slit, with a 15 arcsec length and oriented North–South, which allowed us simultaneous measurements of the object and sky. The object position on the slit was alternated between two locations referred to as the A and B positions. The seeing varied between 0.7 and 1.8 arcsec during the observing runs and the humidity was in the 25–55% range. The automatic guiding mode of the telescope was used for spectra acquisition.

The asteroids were observed in during two observing runs: 28–30 March 2003 and 5 July 2003. The observed objects are summarized in Table 1. We also observed the standard stars SA 98-978, SA 102-1081, SA 105-56, SA 107-684, SA 113-276, SA 115-271, HD 28099, HD 88618 and 16 CyB. Flat-fields and Argon lamp arc images were taken each night and used for data reduction.

Our strategy was to observe all asteroids as close to the zenith as possible. Thus, we managed to observe with an airmass less then 1.6 for all targets except 2181 Fogelin, which we could only observe with an airmass in the 1.7–1.78 range. Science exposures were alternated with standard stars spectra exposures, the latter taken to cover the 1–1.8 airmass range.

In order to obtain a S/N in the 80–150 range, we needed 20–40 min of exposure time, depending on the asteroid magnitude and counting both the effective exposure and CCD camera readout time. This exposure time is unacceptable for a single near-IR spectrum due to the large variations in the atmospheric conditions (a single near-IR spectral exposure is usually no longer than 120 s). In order to obtain the required S/N, we obtained a number of 6–10 A and B exposure pairs (cycles) for both

Table 1
Potential asteroid targets for the Rosetta mission

Object	Date	a (a.u.)	e	i (deg)	Φ (deg)	V (mag)
21 Lutetia	March 30 2003	2.4347	0.1636	3.0645	14.6	11.32
89 Julia	March 30 2003	2.5519	0.1825	16.1437	13.2	11.39
140 Siwa	March 30 2003	2.7365	0.2153	3.1882	21.2	13.72
2181 Fogelin	July 5 2003	2.5918	0.1177	13.0205	11.2	16.59
5480 1989YK8	March 30 2003	3.1366	0.087	6.6717	12.7	16.25

Observation date, semimajor axis, eccentricity, inclination, phase angle and the apparent magnitude are presented for each asteroid.

Table 2
Exposure data for each asteroid

Object	UT (h m s)	Itime (s)	Cycles	Airmass
21 Lutetia	13 35 46	15	8	1.223
21 Lutetia	11 28 17	20	4	1.329
21 Lutetia	15 01 03	15	9	1.414
21 Lutetia	10 20 21	20	3	1.635
89 Julia	10 44 44	40	6	1.561
140 Siwa	07 06 07	120	8	1.000
140 Siwa	07 46 10	120	6	1.016
2181 Fogelin	12 10 35	2×60	4	1.769
2181 Fogelin	12 31 40	2×60	4	1.744
2181 Fogelin	12 55 17	2×60	4	1.740
5480 1989YK8	12 41 01	120	6	1.151
5480 1989YK8	14 36 01	120	6	1.230

The columns show the mean UT value for each series, the individual time for each spectrum (Itime), the number of cycles and the mean airmass of each series.

the asteroids – science exposures – and the standard stars. This constitutes *one series* of observations for each object. Details the science exposures are given in Table 2.

3. Data reduction and results

The major points of our reduction procedure are classic for the near-IR spectroscopy. We started by combining and normalizing flat-fields for each observing night. The resulting flats were later used for the reduction of spectra of both the asteroids and the standard stars. In order to minimize the atmospheric and telescope influence and to eliminate the influence of electronic bias level and the dark current, we subtracted the B position spectra from the A position spectra for each pair of exposures (cycle), in the assumption of quasi-homogeneous sky background during A plus B exposure pair. The result of the subtraction was flat fielded. For each object, we median combined the result of all cycles in each observing series. This technique produces one positive and one negative spectrum on the same image. Next step was the construction of an accurate spatial profile for the extraction of the spectra. The final step was the wavelength calibration.

The Spextool package (the description of the procedures are presented in Cushing et al., 2003) allowed us to perform following steps for both the asteroids and the standard stars: global flat-field and arc construction, possible non-linearity correction, addition of spectra of the same object, spatial profile determination of the spectrum in the image, aperture location, extraction of the spectrum, wavelength calibration and cleaning the spectra. The results are saved in both FITS and ASCII formats, as used by several image processing packages (like IDL, MIDAS and IRAF), respectively, dedicated plot/graphics software (Easyplot, Origin, Dataplot, etc.).

The next step in the process of data reductions was the calculation of the extinction coefficients. The solar analogs spectra were used to find the correspondent extinction coefficient for each wavelength. A "superstar" was created by summing appropriately weighted contributions of the standard stars. The resulting "superstar", corrected for atmospheric extinction, was used to obtain the spectral reflectance of asteroids at different airmasses. Careful choice of the "superstar", combined with several tests of shift between the spectrum of the asteroid and that of the superstar are very important in order to minimize the influence of the terrestrial atmosphere in the 1.4 and 1.9 μm spectral regions. In order to make more readable our spectra, we choose to eliminate these spectral regions. Moreover, the elimination of these spectral regions does not affect the conclusions of this article.

3.1. 21 Lutetia

With an estimated diameter of 95.5 ± 4.1 km – for an IRAS albedo of 0.221 ± 0.020 (Tedesco and Veeder, 1992) – 21 Lutetia belongs to the large asteroid class (diameter $\geqslant 100$ km). Its synodic period has been computed from several lightcurve analysis and the value is 8.17 ± 0.01 h (Zappala et al., 1984). Color analysis of the ECAS data (Zellner et al., 1985) designates the asteroid 21 Lutetia to be part of the *X* complex. Also, global ECAS and IRAS thermal albedo data analysis assign Lutetia to the M taxonomic type (Barucci et al., 1987; Tholen, 1989). The M type asteroids are considered to be part of the core of differentiated asteroids and the parent bodies of metallic meteorites. On the basis of SMASS II spectroscopic data, Bus and Binzel (2002) proposed the new taxonomic class *Xk* for the asteroid 21 Lutetia.

21 Lutetia was observed on UT 2003 March 29 for the entire night. Four series of exposures resulted in four IR spectra with S/N in the 90–140 range. In order to detect possible surface spectral features variations, our observations covered 65% of the synodic period. These spectra are presented in Fig. 1. However, a check of the physical ephemeris of 21 Lutetia revealed a close pole-on geometry of the asteroid, so our spectra are most probably dominated by the contribution of the same surface features on 21 Lutetia. There are no significant spectral features in the spectral region 0.8–2.5 μm and the slightly increasing slope varies around 0.3%.

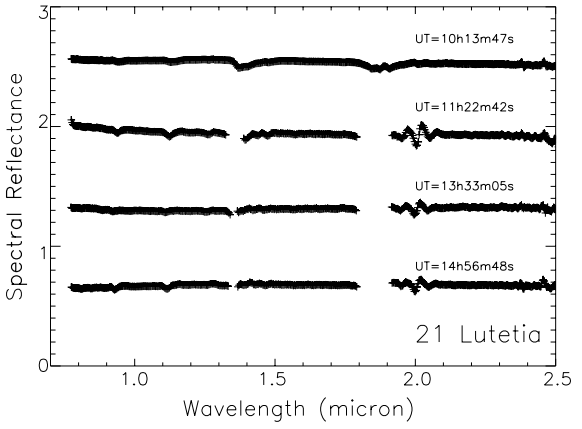

Fig. 1. The spectra of the asteroid 21 Lutetia. The IRTF spectra are offset for clarity and presented in chronological order. The beginning of each series of spectra (UT) was marked on the graph.

The lack of features in the spectrum of 21 Lutetia makes its taxonomic and compositional interpretation difficult. While the high IRAS albedo value of 0.221 leads to the previous M-type classification, we note there is an ambiguity in determining the albedo of Lutetia. An alternate low albedo value of 0.09 has been reported by Zellner et al. (1977) from polarimetric measurements and groundbased radiometric measurements.

In Fig. 2 we compare our measurements of Lutetia with others published in the literature. We found a good match with both SMASS IR data (spectral interval 0.8–1.6 μm) and the 52-color asteroid survey (Bell et al., 1988) spectrophotometric data. We also compare in Fig. 2 all of these Lutetia results with reflectance spectra of meteorites from Gaffey (1976). Our goal is to find which meteorites may be most analogous with Lutetia in terms of near-IR spectral properties. We note the spectrum of Lutetia is most qualitatively similar to the spectrum of the Vigarano meteorite, a CV3 carbonaceous chondrite, while being quite a poor match to the class IIIA iron meteorite Chulafinee. The purpose of our comparison is to note the difficulty of making a non-ambiguous interpretation of the composition of 21 Lutetia.

In Fig. 3 we plot the negative polarization depth versus the inversion angle (Belskaya and Lagerkvist, 1996) for both 21 Lutetia and a sample asteroids and meteorites. The asteroid 21 Lutetia has the largest inversion angle ever observed for the asteroids. The same peculiarly large inversion angle were found in the laboratory for the carbonaceous chondrites of the CV3 and CO3 samples. These types of chondrites are characterized by a low carbon content and thus relatively a larger

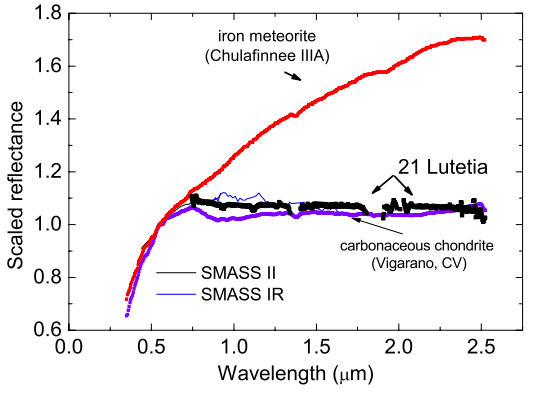

Fig. 2. The average spectrum of the asteroid 21 Lutetia. The SMASS II and SMASS IR data are plotted as solid lines. Our data is in agreement with the SMASSIR data over the 0.75–1.6 μm spectral interval. The comparison with Chulafinnee (iron meteorite) and Vigarano (carbonaceus chondrite) reveal the good match with the IR spectrum associated to carbon rich surfaces.

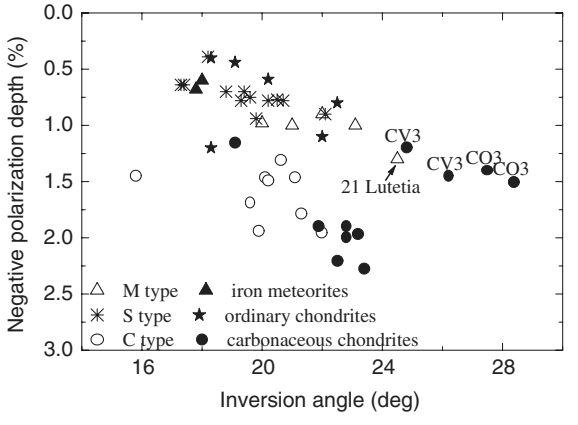

Fig. 3. Diagram of the negative polarization depth and the inversion angle of asteroids and meteorites from Belskaya and Lagerkvist (1996).

albedo when compared to other types (Zellner et al., 1977).

3.2. 89 Julia

The asteroid 89 Julia has an estimated diameter of 151.4 ± 3.1 km, for an IRAS albedo of 0.176 ± 0.007. Photometry of 89 Julia yields a synodic period of 11.387 ± 0.002 h (Schober and Lustig, 1975). Multivariate statistics classified the asteroid as part of the S cluster (Barucci et al., 1987; Tholen, 1989). The mineralogical classification of the S-type asteroids (Gaffey et al., 1993) based on the ECAS data and 52-color spectrophotometric Survey (Bell et al., 1988) data assigns 89 Julia (together with the asteroid 9 Metis) as 'ungrouped' S-asteroids. The main reason of this 'unclassification' is the long wavelength position of the 1 μm feature, which could be the presence of the abundant calcic clinopyroxene component (Gaffey et al., 1993). Based on the SMASS II data, Bus and Binzel (2002) proposed a K cluster membership (derived from the S cluster) for 89 Julia.

The asteroid spectrum was obtained for an effective integration time of 10 min, with a S/N ratio of 90 in both A and B beams. This spectrum presents a significant positive slope in the region 1.1–1.5 μm and a plateau in the 1.7–1.9 μm and 2.2–2.5 μm spectral regions. In Fig. 4 the IR spectrum of Julia was overlapped with the SMASS II spectrum in the 0.78–0.92 μm spectral region. We confirm a broad absorption band at 1 μm, typical of the silicate rich minerals. We also confirm a global trend of the spectral reflectance, which increases in the near-IR. The influence of atmospheric water absorbtion on the spectra is visible around 1.4 and 1.9 μm. The geometry of observations was fairly unfavourable for this asteroid (airmass = 1.56).

In order to calculate the center of 1 μm absorbtion band (designed as Band I in the literature), the continuum was defined between the local maximum of spectral reflectance at 0.76 μm and the small shoulder of the spectrum at 1.27 μm. The spectrum was then continuum subtracted and the result was fitted with an order three polynomial function. We find the center of the feature localized at 1.01 ± 0.06 μm, which is a slightly shorter wavelength than the one found by Gaffey et al. (1993).

3.3. 140 Siwa

140 Siwa is one of the initial targets of the Rosetta mission (departure in January 2003). One of the proposed scenarios (February 2003) suggests keeping this asteroid as a candidate for flyby. This was our motivation to observe it.

An IRAS albedo of 0.068 ± 0.004 for the asteroid 140 Siwa allows the calculation of a diam-

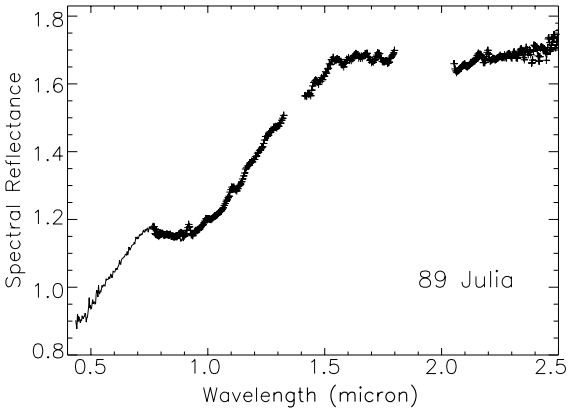

Fig. 4. The spectrum of the asteroid 89 Julia. The IRTF spectrum was overlapped with the SMASS II visible spectrum in the region 0.78–0.92 μm.

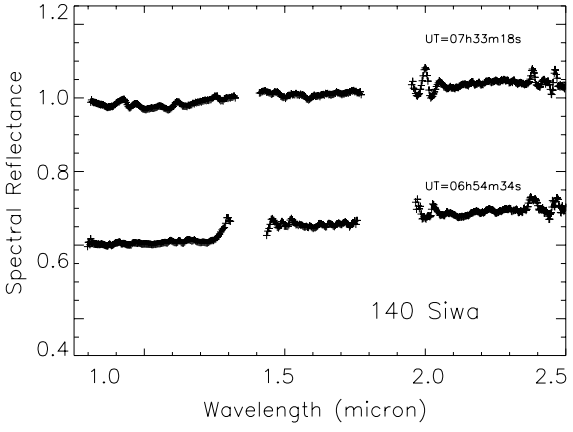

Fig. 5. The spectra of the asteroid 140 Siwa. The spectra were offset for clarity and the UT represents the beginning of each series of exposures.

eter of 109.8 ± 3.0 km. Lightcurve analysis for two runs in 2000 (LeBras et al., 2001) reveals a slow-rotator asteroid; the composite lightcurve presents an amplitude of 0.1 magnitudes and its synodic period was estimated at 18.495 ± 0.005 h.

Two series of near-IR spectra were obtained in March 30, 2003, with the ratio S/N of 50 and 70 (obtained in both A and B beams) for the spectrum obtained at airmass 1.001 and 1.018, respectively, (Fig. 5). The IR spectrum of 140 Siwa does not contain deep absorption features corresponding to mafic minerals. The spectrum slope is slightly positive, with a value 1% (0.8% and 0.7%, respectively), which confirms the slope trend of its spectrum (LeBras et al., 2001). We confirm a typical neutral spectrum of consistent with the a C-type asteroid; the IRAS albedo for 140 Siwa also fits very well the average value of C taxonomic class. The near-IR slope of our spectra is slightly different of those of a typical C-type asteroid but this alone cannot indicate a different mineralogy of the surface.

Fig. 6 shows the computed a global IRTF spectrum for the asteroid 140 Siwa overlapped with SMASS II data (the overlap is only for the 0.7–0.85 μm region). This composite spectrum was compared to meteorite reflectance spectra from the

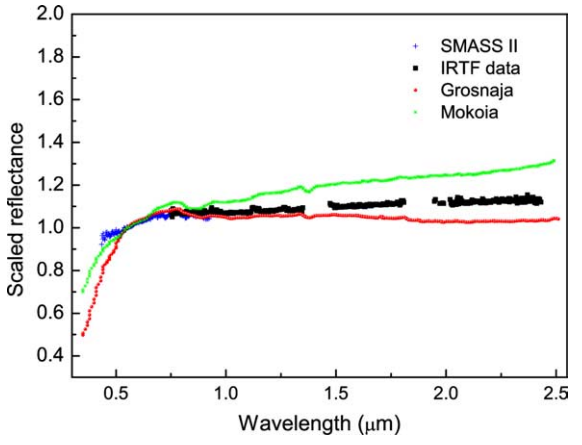

Fig. 6. Cumulated spectral reflectance of the asteroid 140 Siwa obtained during the IRTF run. The spectrum was overlapped with the SMASS II data in the 0.70–0.85 μm spectral region. The spectrum is similar to CV3 meteorites Grosnaja and Mokoia. The surface of 140 Siwa shows similar properties with carbonaceous chondrite meteorites, with a reflectance trend between the curves for the two meteorites.

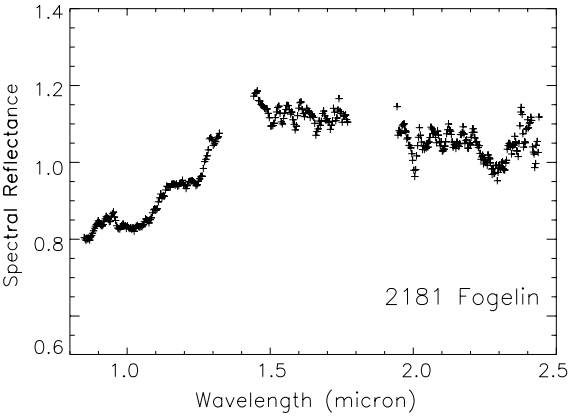

Fig. 7. The spectrum of the asteroid 2181 Fogelin, normalized to 1.275 μm, the maximum of J filter.

Gaffey database. There is no meteorite spectrum that fits our spectrum very well. However, the carbonaceous chondrite meteorites spectra are similar to our spectrum and the asteroid spectral reflectance spans a value in the range of CV3 meteorite class. The nearest spectra are those of Grosnaja and Mokoia meteorites.

3.4. 2181 Fogelin

No physical data are available in the literature for the asteroid 2181 Fogelin. Thus, we can only roughly estimate its diameter. Following the asteroid mass distribution proposed by Kresak (1977) and the H magnitude of 2181 Fogelin, the diameter could be in the 12–18 km range. A second estimate can be made using an empirical relationship between the absolute magnitude, diameter and geometric albedo (Fowler and Chillemi, 1992):

$$\log D = 3.1236 - 0.5 \cdot \log p_v - 0.2 \cdot H. \quad (1)$$

Using an IRAS albedo of 0.05–0.25 we find a 12–22 km diameter for the asteroid.

The observations of 2181 Fogelin were carried out in July, 5, 2003, with the ratio S/N of 80 in both A and B beams. The geometry of observation (airmass = 1.7) was unfavourable. However, the final spectrum is the average of 32 individual spectra, which can alleviate the high airmass problem. The IR spectrum presented in Fig. 7 shows the large

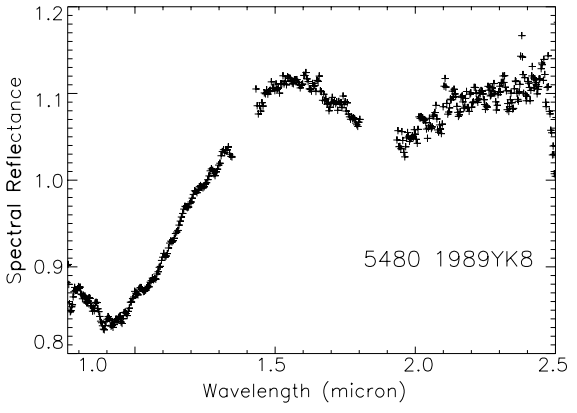

Fig. 8. The spectrum of the asteroid 5480 1989YK8, normalized to 1.275 μm, the maximum of J filter.

broad band absorbtion around 1 μm, typical of mafic minerals. The slightly positive slope in the 1.2–1.5 μm wavelength region doesn't allow us to classify this object as a S-type asteroid. Further observations in the visible region as well as thermal albedo data are necessary to make a taxonomic class assignment for this asteroid.

3.5. 5480 1989YK8

There are no previous photometric or spectroscopic data available for the asteroid 5480 1989YK8. The same methods used for 2181 Fogelin have been used to compute its theoretical diameter. The diameter spans the 13–20 km range (following Kresak, 1977) and 13–31 km following the diameter empirical formula (1), used with IRAS albedos in the 0.05–0.25 range.

The asteroid was observed on March, 30, 2003 and the final spectrum S/N ratio is around 100 for the A and B positions in the slit. The analysis of the 0.8–2.3 μm region reveals an absorption band around 1 μm (Fig. 8). The global tendency in near-IR could justify a S-type asteroid classification; however, a visible spectrum and thermal albedo data are necessary for a taxonomical assignment.

4. Conclusions

Five asteroids potential targets for the Rosetta mission have been observed in the 0.8–2.5 μm spectral range: 21 Lutetia, 89 Julia, 140 Siwa, 2181 Fogelin and 5480 (1989YK8). We confirm the flat near-IR spectrum of 21 Lutetia. The near-IR spectrum of 89 Julia contains features confirming the initial idea that it belongs to the 'heated' bodies, possible to the S or K taxonomic class. A value 1.01 ± 0.06 μm was found for the center of the Band I. The asteroid 140 Siwa spectrum presents a slightly positive slope and there are no major mineralogical signatures; we confirm the assignment of the asteroid as an 'unheated' asteroid.

The small asteroids 2181 Fogelin and 5480 (1989YK8) were observed spectroscopically for the first time. Our data shows the presence of a large (and weak) absorption band around 1 μm for both asteroids; new observations in visible and infrared are necessary to draw a reliable conclusion concerning their surface mineralogy.

The remote observations between IRTF and Observatoire de Paris-Meudon proved to be a robust and handy observing technique. It offered full access to the command line of the spectrograph and to several telescope controls (focus, tracking, etc.). We consider our observing program entirely accomplished without any discernable difference in the typical amount of spectra obtained in remote observations mode versus the local observing mode.

Acknowledgements

The authors are grateful to Paul Hardersen for useful comments that improved our article. We are indebted to Tony Denault who answered many questions prior to our runs about the Polycom system and exporting of X-windows for SpeX and guiding system, to Miranda Hawarden-Ogata for the administration system support and to Paul Sears and Bill Golish, the telescope operators during the remote observing runs.

References

Barucci, M.A., Doressoundiram, A., Fulchignoni, M., Florczak, M., Lazzarin, M., Angeli, C., 1998. P&SS 46, 75–82.
Barucci, M.A., Capria, M.T., Coradini, A., Fulchignoni, M., 1987. Icar 72, 304–324.

Bell, J.F, Hawke, B.R., Owensby P.D, Gaffey, M.J., 1988. The 52-color asteroid survey; final results and interpretation. Lunar Planet. Sci. XIX.

Belskaya, I., Lagerkvist, C.-I., 1996. P&SS 44, 783.

Birlan, M., Binzel, R.P., 2002. Paris Observatory Remote Observing January–May 2002: Sharing the Experience to Educational Astronomy, Global Hands-On Universe Conference Proceedings, Paris, July.

Bus, S.J., Binzel, R.P., 2002. Icar 158, 146.

Cushing, M.C., Vacca, W.D., Rayner, J.T., 2003. Spextool: a spectral extraction package for SpeX, a 0.8–5.5 μm cross-dispersed spectrograph, PASP (in press), http://irtf-web.ifa.hawaii.edu/Facility/spex/.

Fornasier, S., Barucci, M.A., Binzel, R.P., et al., 2003. A&A 398, 327.

Fowler, J.W., Chillemi, J.R., 1992. IRAS asteroid data processing. In: Tedesco, E.F., Veeder, G.J., Fowler, J.W., Chillemi, J.R. (Eds.), The IRAS Minor Planet Survey. Technical Report PL-TR-92-2049, Phillips Laboratory, Hanscom AF Base, MA.

Gaffey, M.J., 1976. JGR 81, 905.

Gaffey, M.J., Burbine, T.H., Piatek, J.L., Reed, K.L., Chaky, D.A., Bell, J.F., Brown, R.H., 1993. Icar 106, 573.

Kresak, L., 1977. BAICz, n. 28, 82.

Le Bras, A., Dotto, E., Fulchignoni, M., Doressoundiram, A., Barucci, M.A., Le Mouelic, S., Forni, O., Quirico, E., 2001. A&A 379, 660.

Schober, H.J., Lustig, G., 1975. Icar 25, 339.

Tedesco, E.F., Veeder, G.J., 1992. IMPS albedos and diameter catalog(FP102). In: Tedesco, E.F., Veeder, G.J., Fowler, J.W., Chillemi, J.R., The IRAS Minor Planet Survey. Technical Report PL-TR-92-2049, Phillips Laboratory, Hanscom AF Base, MA.

Tholen, D., 1989. Asteroid taxonomic classifications. In: Asteroids II. University of Arizona Press, AZ, pp. 1139–1150.

Zappala, V., DiMartino, M., Knezevic, Z., Djurasevic, G., 1984. A&A 130 (1), 208.

Zellner, B., Tholen, D.J., Tedesco, E.F., 1985. Icar 61, 355.

Zellner, B., Leake, M., LeBerte, T., Duseaux, M., Dollfus, A., 1977. The asteroid albedo scale. II. Laboratory polarimetry of meteorites. In: Proceedings of the Lunar Science Conference, 8th ed. Pergamon Press, Oxford, pp. 1091–1110.